

AD-A114 982

AEROSPACE CORP EL SEGUNDO CA LAB OPERATIONS

F/G 7/4

ABSOLUTE RATE COEFFICIENTS FOR F + H(2) AND F + D(2) AT T = 295--ETC(U)

MAY 82 R F HEIDNER, J F BOTT, C E GARDNER

F04701-81-C-0082

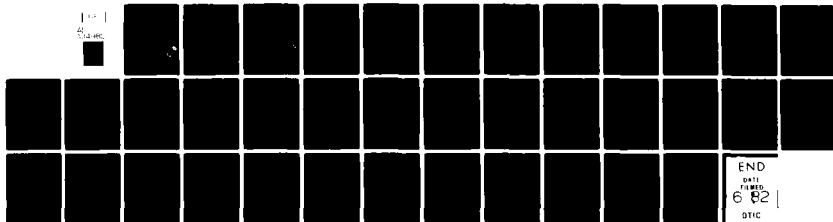
UNCLASSIFIED

TR-0082(2930-01)-1

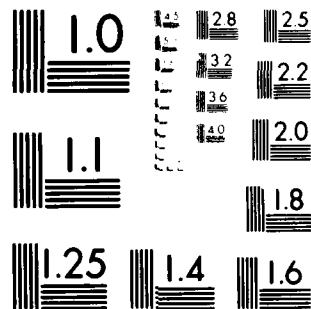
SD-TR-82-21

NL

1 of 1  
1 of 1



END  
DATE  
FOR INFO  
6 82  
DTIC



MICROCOPY RESOLUTION TEST CHART  
NATIONAL BUREAU OF STANDARDS-1963-A

AD A114982

REPORT SD-TR-82-21

12

**Absolute Rate Coefficients  
for  $F + H_2$  and  $F + D_2$   
at  $T = 295 - 765 \text{ K}$**

**R. F. HEIDNER III, J. F. BOTT,  
C. E. GARDNER, and J. E. MELZER  
Laboratory Operations  
The Aerospace Corporation  
El Segundo, Calif. 90245**

**5 May 1982**

**APPROVED FOR PUBLIC RELEASE;  
DISTRIBUTION UNLIMITED**

**Prepared for  
SPACE DIVISION  
AIR FORCE SYSTEMS COMMAND  
Los Angeles Air Force Station  
P.O. Box 92000, Worldway Postal Center  
Los Angeles, Calif. 90009**

**DTIC  
EXTRACTED  
MAY 20 1982  
H**

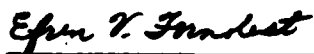
**DTIC FILE COPY**

**82 05 28 001**

This report was submitted by The Aerospace Corporation, El Segundo, CA 90245, under Contract No. FO4701-81-C-0082 with the Space Division, Deputy for Technology, P.O. Box 92960, Worldway Postal Center, Los Angeles, CA 90009. It was reviewed and approved for The Aerospace Corporation by W. P. Thompson, Director, Aerophysics Laboratory. Lt E. V. Fornoles, SD/YLXT, was the project officer for the Mission-Oriented Investigation and Experimentation (MOIE) Program.

This report has been reviewed by the Public Affairs Office (PAS) and is releasable to the National Technical Information Service (NTIS). At NTIS, it will be available to the general public, including foreign nations.

This technical report has been reviewed and is approved for publication. Publication of this report does not constitute Air Force approval of the report's findings or conclusions. It is published only for the exchange and stimulation of ideas.

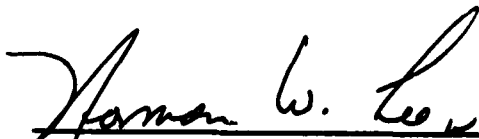


Efren V. Fornoles, 1st Lt, USAF  
Project Officer



Florian P. Meinhardt, Lt Col, USAF  
Director of Advanced Space Development

FOR THE COMMANDER



Norman W. Lee, Jr., Colonel, USAF  
Deputy for Technology

UNCLASSIFIED

SECURITY CLASSIFICATION OF THIS PAGE (When Data Entered)

REPORT DOCUMENTATION PAGE		READ INSTRUCTIONS BEFORE COMPLETING FORM										
1. REPORT NUMBER SD-TR-82-21	2. GOVT ACCESSION NO. AD-A114982	3. RECIPIENT'S CATALOG NUMBER										
4. TITLE (and Subtitle)  ABSOLUTE RATE COEFFICIENTS FOR F + H <sub>2</sub> AND F + D <sub>2</sub> AT T = 295-765 K		5. TYPE OF REPORT & PERIOD COVERED										
7. AUTHOR(s)  R. F. Heidner III, J. F. Bott, C. E. Gardner, and J. E. Melzer		6. PERFORMING ORG. REPORT NUMBER TR-0082(2930-01)-1										
9. PERFORMING ORGANIZATION NAME AND ADDRESS  The Aerospace Corporation El Segundo, Calif. 90245		8. CONTRACT OR GRANT NUMBER(s)  F04701-81-C-0082										
11. CONTROLLING OFFICE NAME AND ADDRESS  Space Division Air Force Systems Command Los Angeles, Calif. 90009		10. PROGRAM ELEMENT, PROJECT, TASK AREA & WORK UNIT NUMBERS										
14. MONITORING AGENCY NAME & ADDRESS (if different from Controlling Office)		12. REPORT DATE 5 May 1982										
		13. NUMBER OF PAGES 33										
		15. SECURITY CLASS. (of this report)  Unclassified										
		15a. DECLASSIFICATION/DOWNGRADING SCHEDULE										
16. DISTRIBUTION STATEMENT (of this Report)  Approved for public release; distribution unlimited.												
17. DISTRIBUTION STATEMENT (of the abstract entered in Block 20, if different from Report)												
18. SUPPLEMENTARY NOTES												
19. KEY WORDS (Continue on reverse side if necessary and identify by block)												
<table border="0"> <tr> <td>Absolute rate coefficients</td> <td>Fluorine atoms</td> </tr> <tr> <td>Arrhenius equations</td> <td>Infrared chemiluminescence</td> </tr> <tr> <td>Chemical lasers</td> <td>Isotope effects</td> </tr> <tr> <td>Cold reaction pumping</td> <td>Multiphoton dissociation</td> </tr> <tr> <td></td> <td>Time-resolved spectroscopy</td> </tr> </table>			Absolute rate coefficients	Fluorine atoms	Arrhenius equations	Infrared chemiluminescence	Chemical lasers	Isotope effects	Cold reaction pumping	Multiphoton dissociation		Time-resolved spectroscopy
Absolute rate coefficients	Fluorine atoms											
Arrhenius equations	Infrared chemiluminescence											
Chemical lasers	Isotope effects											
Cold reaction pumping	Multiphoton dissociation											
	Time-resolved spectroscopy											
20. ABSTRACT (Continue on reverse side if necessary and identify by block number) The rate coefficients of the F + H <sub>2</sub> and F + D <sub>2</sub> reactions must be accurately known over a wide temperature range if the HF and DF chemical lasers are to be properly modeled. Although the pulsed and cw chemical lasers operate at elevated temperatures (500 to 2000 K), no absolute rate data exist for T > 400 K. Extension of the infrared multiphoton dissociation-infrared fluorescence technique permitted the following Arrhenius equations to be determined between 295 and 765 K:												

DD FORM 1473  
(FACSIMILE)

UNCLASSIFIED

SECURITY CLASSIFICATION OF THIS PAGE (When Data Entered)

UNCLASSIFIED

SECURITY CLASSIFICATION OF THIS PAGE(When Data Entered)

19. KEY WORDS (Continued)

20. ABSTRACT (Continued)

$k_F + H_2 = (1.3 \pm 0.25) \times 10^{14} \exp[-(1182 \pm 100)/RT]$ ;  $k_F + D_2 = (6.4 \pm 2.2) \times 10^{13} \exp[-(1200 \pm 142)/RT]$ ;  $k_F + H_2/k_F + D_2 = (2.1 \pm 0.8) \exp[(18 \pm 250)/RT]$ .

UNCLASSIFIED

SECURITY CLASSIFICATION OF THIS PAGE(When Data Entered)

## PREFACE

The authors gratefully acknowledge very productive discussions and information exchange with Professor P. L. Houston. Similarly, we wish to thank Dr. J. Warnatz for communicating the results cited in Ref. 29. Numerous discussions with Dr. N. Cohen have been extremely valuable, and we thank him for permission to use his transition state theory results. Mrs. K. L. Foster performed the NEST computer calculations, and Mr. T. M. El-Sayed contributed to the latter stages of the project.



Accession For	
NTIS GRA&I	<input checked="checked" type="checkbox"/>
DTIC TAB	<input type="checkbox"/>
Unannounced	<input type="checkbox"/>
Justification	
By	
Distribution/	
Availability Codes	
Dist	Avail and/or Special
A	

## CONTENTS

PREFACE.....	1
I. INTRODUCTION.....	9
II. EXPERIMENTAL APPARATUS AND PROCEDURE.....	11
III. DATA ANALYSIS.....	15
IV. RESULTS.....	23
V. DISCUSSION.....	29
VI. CONCLUSIONS.....	35
REFERENCES.....	37

MISSING PAGE BLANK-NOT FILMED



## FIGURES

1.	Multiphoton dissociation--infrared fluorescence apparatus.....	12
2	Time-resolved infrared chemiluminescence trace.....	14
3.	$\Delta\tau_f^{-1}/\Delta[H^2]$ vs $1/T$ and $\Delta\tau_f^{-1}/\Delta[D_2]$ vs $1/T$ .....	19
4.	Inverse rise times $\tau_r^{-1}$ as a function of temperature.....	24
5.	Temperature dependence of the absolute reaction rates.....	27

PRECEDING PAGE BLANK-NOT FILMED

# TABLES

I. Numerical modeling results for representative conditions of $5.4 \times 10^{-11}$ mol/cm <sup>3</sup> of F in Ar + H <sub>2</sub> at a total pressure of 5.2 Torr.....	20
II. Absolute rate coefficients as a function of temperature.....	25
III. Absolute temperature-dependent rate coefficients for F + H <sub>2</sub> → HF <sup>†</sup> + H.....	30
IV. Absolute and relative temperature-dependent rate coefficients for F + D <sub>2</sub> → DF <sup>†</sup> + D.....	31

PRECEDING PAGE BLANK-NOT FILMED

## I. INTRODUCTION

In a recent publication,<sup>1</sup> the absolute rates of the reactions  $F + H_2$  and  $F + D_2$  were studied at  $T = 295$  K. The results for  $F + H_2$  were in very good agreement with earlier studies performed with a variety of experimental techniques. The lack of previous absolute rate data for  $F + D_2$  was noted; however, the ratio of the rates for  $H_2$  and  $D_2$  was in excellent agreement with earlier relative measurements. These earlier measurements have been extensively reviewed.<sup>2-5</sup>

(The extension of the infrared multiphoton dissociation-infrared chemiluminescence technique to elevated temperatures permitted us to derive a set of temperature-dependent rate coefficients for both the  $F + H_2$  and  $F + D_2$  chemical reactions.) Experimental constraints limited the upper temperature range to  $\sim 750$  K; however, no previous absolute data have been reported for  $T > 397$  K. These data and the data reported in a concurrent study by Wurzburg and Houston<sup>6</sup> at  $T = 190-373$  K provide a greatly improved data set for comparison to theory and for modeling of the HF and DF chemical lasers. A number of classical trajectory calculations<sup>7-9</sup> on semi-empirical potential energy surfaces have yielded Arrhenius plots for the  $F + H_2(D_2)$  reactions. Recently, Cohen<sup>10</sup> performed extensive parameter variations in a transition state theory description of the temperature dependence for these two processes. These theoretical treatments provide valuable modeling data, since real HF and DF chemical lasers operate at elevated temperatures and any kinetic model that describes them must incorporate accurate  $T$ -dependent parameters for the  $F + H_2$  and  $F + D_2$  reactions. Calculations on electron-beam-initiated  $H_2-F_2-O_2$

mixtures indicate that more than 60% of the laser energy can be emitted at active medium temperatures between 500 and 2000 K.<sup>11</sup> In principle, the modeling of these lasers requires not only thermal rate coefficients, but cross sections for translationally-hot F (and H) atoms,<sup>12</sup> since these laser systems are generally not buffered by an inert gas. Although the data presented here are for thermalized reaction rates as a function of temperature, they may guide the calculation of reaction cross sections vs relative velocity for these two reactions.

## II. EXPERIMENTAL APPARATUS AND PROCEDURE

The details of the apparatus are given in Ref. 1. The F atoms were produced by the infrared multiphoton dissociation of  $\text{SF}_6$  and the rate of the  $\text{F} + \text{H}_2(\text{D}_2)$  reactions monitored by the time-dependent chemiluminescence from  $\text{HF}^\dagger(\text{DF}^\dagger)$ . Partial pressures of Ar buffer gas,  $\text{SF}_6$  and  $\text{H}_2(\text{D}_2)$  were deduced from molar flow rates of the various gases and the total system pressure. The variable-temperature flow cell required for the present experiment was constructed of 45-mm i.d. quartz with Infrasil windows (37.5-mm diam) fused onto 2-cm-long side ports (Fig. 1). The cell was enclosed in a cylindrical, ceramic-fiber, molded oven (Watlow Co.) with the cell windows emerging from the oven walls. In principle, the maximum operating temperature for this arrangement is  $\sim 1200$  K. The cell temperature was measured with a digital thermocouple (Omega Engineering), which used a chromel-alumel junction encased in a stainless-steel sheath. At the Ar buffer pressure of 5 Torr, when the thermocouple probe was moved across the diameter of the flow tube, negligibly small temperature variations ( $\pm 3$  K) were produced over the entire temperature range studied. The extremely small gas flows used prevent serious systematic errors in temperature determination.<sup>13</sup>

Infrared chemiluminescence from the  $\text{F} + \text{H}_2(\text{D}_2)$  reactions was collected by  $\text{CaF}_2$  lenses (f/1) arranged as a compound microscope. After the radiation passed through an appropriate interference filter, it was refocused onto a 77 K InSb detector (Texas Instruments). The detected signal was further increased ( $\times 2$ ) by the use of a spherical Al backing mirror.

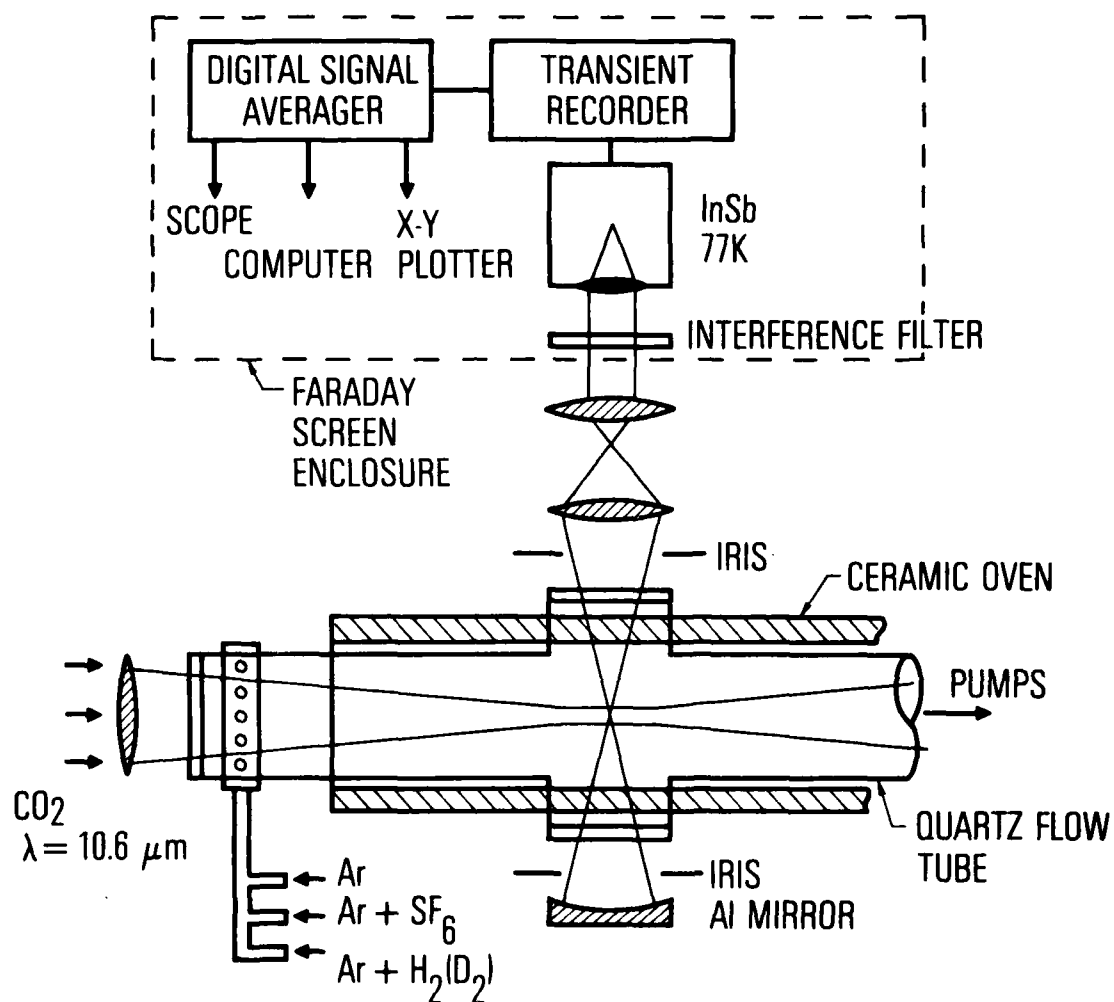


Fig. 1. Multiphoton dissociation--infrared fluorescence apparatus.

The two irises indicated in Fig. 1 helped reduce the amount of blackbody radiation collected from the oven assembly. Although the cell windows remained much cooler than the cell walls, blackbody emission from the Infrasil windows prevented measurements at  $T > 800$  K. This problem was somewhat worse for DF, because the bandpass filter sampled longer wavelengths than the equivalent filter for HF. The signal was processed with a Biomation 805 transient recorder and accumulated in a Nicolet 1072 digital signal averager. A typical trace is illustrated in Fig. 2. All data represent the sum of eight laser pulses.

Considerable effort was expended to explain and remove the anomalously large quenching of  $\text{HF}^+$  and  $\text{DF}^+$  observed during the room-temperature studies.<sup>1</sup> As predicted, a major fraction of this quenching resulted from an  $\text{H}_2\text{O}$  impurity in the bulk gases and was effectively removed by passing the Ar and the Ar +  $\text{H}_2(\text{D}_2)$  mixtures through a low-pressure, glass-wool packed trap held at 77 K.

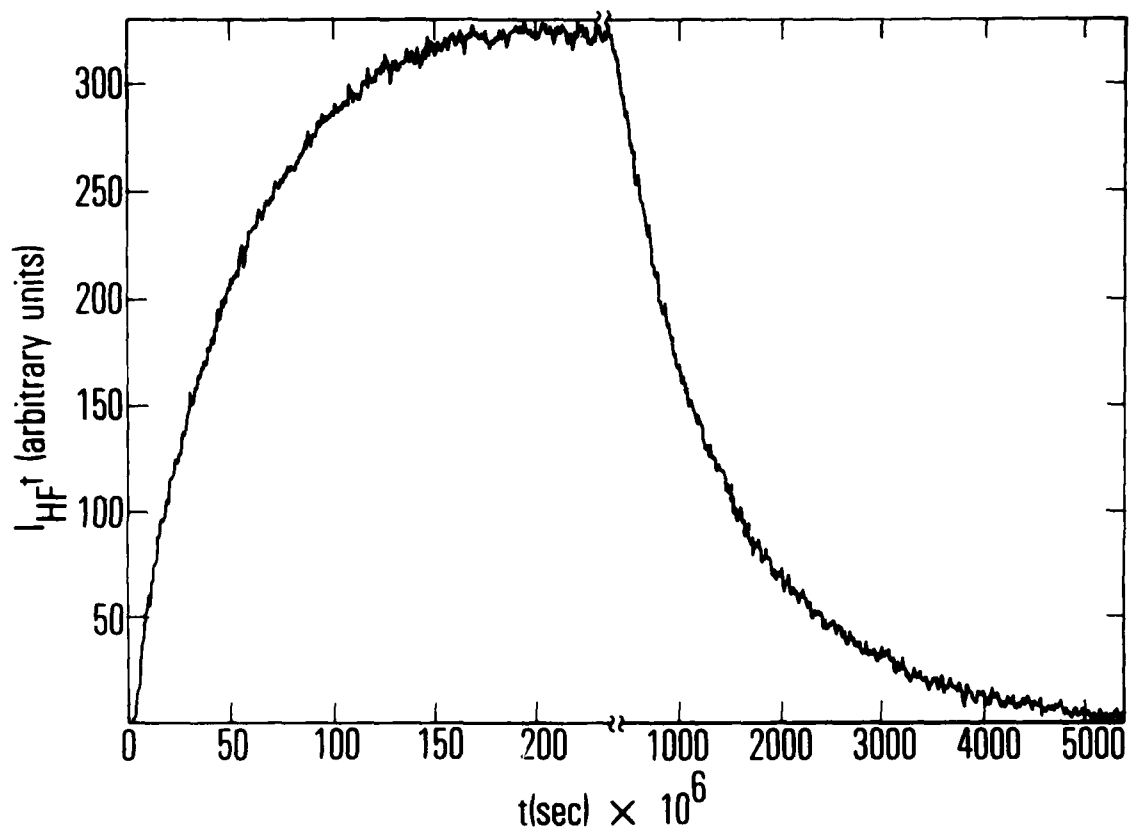


Fig. 2. Time-resolved infrared chemiluminescence trace. Channels 1 through 512, 0.5  $\mu\text{s}/\text{channel}$ ; channels 513 through 1024, 10  $\mu\text{s}/\text{channel}$ . Partial pressures:  $\text{SF}_6 = 33 \text{ mTorr}$ ,  $\text{H}_2 = 24.3 \text{ mTorr}$ ,  $\text{Ar} = 3.87 \text{ Torr}$ .  $T = 295^\circ\text{K}$ .



### III. DATA ANALYSIS

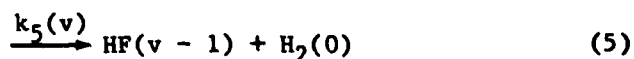
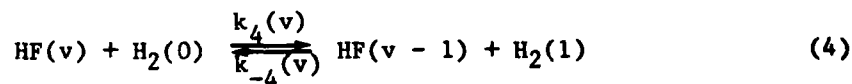
In our earlier study,<sup>1</sup> we outlined the procedure for relating chemiluminescence intensity from product  $\text{HF}^\dagger(\text{DF}^\dagger)$  to the disappearance of the F-atom reactant. The initial vibrational populations are produced by Reactions (1) and (2):



Clearly, the intensity is given by

$$I(t) = \sum_v A_v [\text{HF}(v)] \quad (3)$$

where  $A_v$  is the radiative lifetime of the  $v$ th vibrational level. The product vibrational levels are removed by diffusion, radiation, and impurity quenching, but primarily these levels are removed by the  $\text{H}_2$  (or  $\text{D}_2$ ) that is in relatively large concentration:



Ordinarily, the kinetic system represented by Eqs. (4) and (5) produces a double-exponential decay<sup>14</sup> of the fluorescence from HF. Unlike the conventional laser-induced fluorescence experiment where  $\text{HF}(0)$  and  $\text{H}_2(0)$  are

uniformly distributed in the cell, the present experiment creates  $\text{HF}^\dagger$  initially in the 2 to 3-mm-diam focal caustic of the laser. The  $\text{HF}(\text{v})$  and  $\text{H}_2(1)$  encounter a large excess of  $\text{H}_2(0)$  as they rapidly diffuse out of the focal volume. Since  $[\text{H}_2(1)]/[\text{H}_2(0)]$  remains small, the equilibrium defined by Eq. (4) is never established. Therefore, the effective rate coefficient for removal of  $\text{HF}(\text{v})$  by  $\text{H}_2(0)$  in this experiment is  $k_4(\text{v}) + k_5(\text{v})$ .

An approximate analytic solution of the time derivative of  $I(t)$  was developed in Ref. 1:

$$I(t) = \frac{C_1 k_1 [\text{H}_2] [F]_0}{k_1 [\text{H}_2] - (k_4(1) [\text{H}_2] + C_2)} \left\{ \exp [-(k_4(1) [\text{H}_2] + C_2)t] - \exp(-k_1 [\text{H}_2]t) \right\} \quad (6)$$

where  $C_1 = [\Sigma A_v k_1(\text{v})]/k_1$  and  $C_2 = \tau_{\text{RAD}}^{-1} + \tau_{\text{DIFF}}^{-1}$ . The term  $C_2$  describes the removal of  $\text{HF}^\dagger$  in the complete absence of collisional quenching. Within the approximations made for this kinetic scheme,<sup>1</sup> the rise time of the fluorescence intensity  $\tau_r$  is directly related to the overall rate coefficient  $k_1$  by  $\tau_r^{-1} = (k_1 [\text{H}_2])$  and the decay time  $\tau_f$  can be expressed as  $\tau_f^{-1} = (k_4(1) [\text{H}_2] + C_2)$ . A simplified working expression for the fluorescence intensity is given by Eq. (7):

$$I(t) = \frac{C_1 \tau_r^{-1} [F]_0}{\tau_r^{-1} - \tau_f^{-1}} \left[ \exp\left(\frac{-t}{\tau_f}\right) - \exp\left(\frac{-t}{\tau_r}\right) \right] \quad (7)$$

For the earlier room temperature results, this analytic equation was quantitatively tested with the use of The Aerospace Corporation's numerical modeling code, NEST<sup>15</sup>. In that study, computer modeling calculations indicated that as

long as  $\tau_r \ll \tau_f$ , then  $\tau_r^{-1} = k_1[H_2]$  is a good approximation. For comparison with the data of the present study, the modeling calculations were performed at several temperatures between 200 and 1000 K. Literature values were used for the Einstein coefficients,<sup>16</sup> the relative distributions over the product vibrational states,<sup>17,18</sup> and the rate coefficients for HF(v) deactivation by H<sup>19</sup> and H<sub>2</sub>.<sup>20,21</sup> The V-R, T deactivation of HF(v) by HF was assumed to occur by single-quantum processes with rate coefficients scaling as  $v^{2.6}$  for the higher vibrational levels.<sup>22</sup> The temperature dependence used for HF(1)-HF relaxation was taken from Ref. 5. The calculations included losses caused by radiative decay but not by diffusion.

The calculated fluorescence traces were fitted to  $[\exp(-t/\tau_f) - \exp(-t/\tau_r)]$  and  $\tau_r$  and  $\tau_f$  were determined in the same manner as in the analysis of the actual experimental data. Calculations were performed for several H<sub>2</sub> concentrations at the same temperature, and the values of  $\tau_r^{-1}$  and  $\tau_f^{-1}$  were plotted vs H<sub>2</sub> concentration. It was found that  $\tau_r^{-1} = k_1[H_2]$  within the accuracy of the curve fitting as long as there is sufficient H<sub>2</sub> so that it will not be depleted during the reaction. The rise-times were not sensitive to changes in the relative product distributions or the Einstein coefficients.

The calculated fluorescence traces decreased from their maximum to about  $e^{-1}$  of their maximum with approximately exponential decay rates. A plot of decay rates at 700 K vs  $[H_2]$  had a slope of  $3.3 \times 10^{11}$  cm<sup>3</sup>/mol-sec compared with the value of  $5.4 \times 10^{11}$  cm<sup>3</sup>/mol-sec used for  $k_4(1)$ , the rate coefficient for HF(1) deactivation by H<sub>2</sub>. Thus, the H<sub>2</sub> quenches the total fluorescence of

the highly excited HF with a quenching rate  $\sim 0.55$  times the deactivation rate of HF(1) by H<sub>2</sub>.

The decay times obtained from the modeling calculations are longer than the measured values; the H<sub>2</sub> quenching rate of the total fluorescence is about twice as fast as predicted by the modeling calculations. An experimental explanation could be low-level impurities of H<sub>2</sub>O in H<sub>2</sub> although care has been taken to avoid such impurities. Other effects, such as diffusion out of the observed volume or deactivation by SF<sub>6</sub> or SF<sub>6</sub> fragments, would not be proportional to the H<sub>2</sub> concentration and would not contribute to the apparent quenching rate of the fluorescence by H<sub>2</sub>. The source of the discrepancy may also be the computer model. The modeling calculations were performed with single-quantum processes for the deactivation of HF(v) by HF and H<sub>2</sub>. A study by Douglas and Moore<sup>22</sup> indicated that HF(4) is deactivated by HF in a single-quantum process. Multi-quantum deactivation of HF(v) by H<sub>2</sub> would bring the modeling calculations into better agreement with the experimental data but would not completely resolve the discrepancy.

In Fig. 3(a), we have plotted the values of  $\Delta\tau_f^{-1}/\Delta[H_2]$  obtained from the experimental data and from the computer modeling calculations vs  $1/T$  (these latter values are the slopes of decay rates  $\tau_f^{-1}$  plotted vs [H<sub>2</sub>] concentration at a constant temperature). For comparison with these data, the values of  $k_4(v = 1)$  are also plotted. The expected value of  $\Delta\tau_f^{-1}/\Delta[H_2]$  is  $k_4(v = 1)$  if  $k_4(v)$  has a particular  $v$  dependence.<sup>1</sup> In Table I the results of the modeling calculations performed at five different temperatures are listed. These results indicate that  $\Delta\tau_r^{-1}/k_1\Delta[H_2] = 0.99 \pm 0.03$ , which is within the

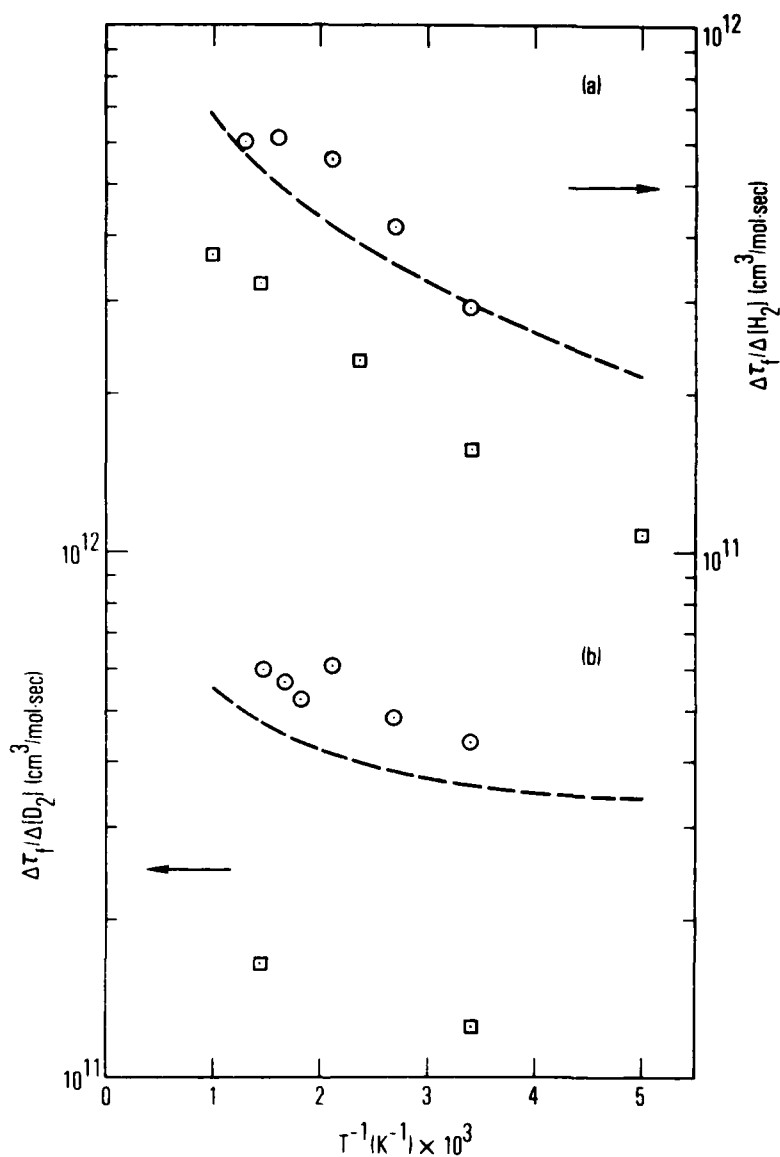


Fig. 3. (a)  $\Delta\tau_f^{-1}/\Delta[\text{H}_2]$  vs  $1/T$ ;  $\odot$  present experimental data obtained from mixtures of Ar and  $\text{H}_2$ ;  $\square$  numerical modeling results (see text); ---- values of  $k_4(1)$  used in the numerical modeling. (b)  $\Delta\tau_f^{-1}/\Delta[\text{D}_2]$  vs  $1/T$ ;  $\odot$  present experimental data obtained from mixtures of Ar and  $\text{D}_2$ ;  $\square$  numerical modeling results (see text); ---- values of  $k_4(1)$  used in the numerical modeling.

TABLE I. Numerical modeling results for representative conditions of  $5.4 \times 10^{-11}$  mol/cm<sup>3</sup> of F in Ar + H<sub>2</sub> at a total pressure of 5.2 Torr.

Temp (K)	$\Delta\tau_r^{-1}/k_1\Delta[H_2]$	$\Delta\tau_f^{-1}/k_4(1)\Delta[H_2]$
200	1.00	0.50
295	0.98	0.53
450	0.98	0.58
700	1.02	0.60
1000	<u>0.97</u>	<u>0.55</u>
Average $0.99 \pm 0.03$		Average $0.55 \pm 0.05$

accuracy of the graphical data reduction. The values of  $\Delta\tau_f^{-1}/k_4(1)\Delta[H_2]$  are close to  $0.55 \pm 0.05$  over the entire temperature range.

Modeling calculations performed for the  $F + D_2$  experimental conditions indicated that  $\tau_r^{-1} = k_2[D_2]$  is a good approximation. However, the discrepancy between the calculated values of  $\Delta\tau_f^{-1}/\Delta[D_2]$  and the experimental values shown in Fig. 3(b) is even larger than the discrepancy for the  $F + H_2$  data in Fig. 3(a). The  $F + D_2$  reaction produces  $DF(v)$   $v \leq 4$  compared with vibrational levels  $v \leq 3$  produced in the  $F + H_2$  reaction, so the numerical modeling of the  $F + D_2$  experiments is even more dependent on the assumption of single-quantum transitions and the  $v$  dependence of the  $DF$  relaxation rate coefficients.

The multiphoton dissociation process is affected by both pressure and temperature. Our experiments are performed at a constant Ar buffer pressure of 5 Torr. Bado and van den Bergh<sup>23</sup> found a very small effect of Ar pressure on the  $SF_6$  dissociation yield at room temperature. We are not concerned with the question of whether the multiphoton dissociation is collisionless in our experiment. The low intensity absorption by  $SF_6$  at the P(20)  $CO_2$  laser line has been studied at elevated temperature by Nowak and Lyman.<sup>24</sup> The absorption coefficient drops rather sharply between 500 and 1000 K as a result of red-shifting of the spectrum. The multiphoton dissociation spectrum is known to be red-shifted from the absorption spectrum, primarily for this reason. Thus, the optimum P-branch line for  $SF_6$  multiphoton dissociation certainly shifts to higher  $J$  as temperature is increased. If studies at  $T > 800$  K are pursued in an improved geometry that limits background interference, these phenomena may be important experimental considerations.

In our earlier paper,<sup>1</sup> we argued that the F atoms were translationally equilibrated by the excess of Ar to H<sub>2</sub> (>50 to 1) before reaction with H<sub>2</sub>. In addition, all available evidence suggests that the F atoms are produced with very little excess translational energy from the multiple photon dissociation of SF<sub>6</sub>. The question of electronic equilibrium was not considered. In Sec. V, the status of the work on the relative reactivities of F(<sup>2</sup>P<sub>1/2</sub>) and F(<sup>2</sup>P<sub>3/2</sub>) is reviewed. Although we know of no experimental data for the electronic quenching of F(<sup>2</sup>P<sub>1/2</sub>) by Ar, data exist for Cl(<sup>2</sup>P<sub>1/2</sub>) quenching.<sup>25</sup> In the case of Cl(<sup>2</sup>P<sub>1/2</sub>) where the spin-orbit splitting is 881 cm<sup>-1</sup>, the quenching coefficient by Ar is  $(1.1 \pm 0.3) \times 10^{-12}$  cm<sup>3</sup>/molecule-sec. Although the quenching of F(<sup>2</sup>P<sub>1/2</sub>) by Ar is expected to be faster since the spin-orbit splitting is only 404 cm<sup>-1</sup>, the presence of these two thermally accessible states is cause for concern.



#### IV. RESULTS

With the use of the information tabulated in Table I, we can ascertain whether the analytic equations (6) and (7) are valid for experimental fluorescence traces. The slopes of the experimental  $\tau_f^{-1}$  vs  $[H_2]$  and  $[D_2]$  curves are plotted vs  $1/T$  in Fig. 3 as are the slopes of the NEST-simulated  $\tau_f^{-1}$  vs  $[H_2]$  and  $[D_2]$  curves. Removal of  $H_2O$  from the Ar and Ar +  $H_2(D_2)$  flows was the primary cause of the improved agreement compared with our original study. Nevertheless, there is substantial disagreement between experiment and model. No experimental data are available for  $HF(v = 2 \text{ and } 3)$  or  $DF(v = 2, 3, \text{ and } 4)$  quenching at high temperatures by  $H_2$  and  $D_2$ , respectively. Recent measurements at  $T = 200$  and  $295 \text{ K}^{22}$  indicate that the vibrational scaling of these quenching rates is rather insensitive to temperature. As a first approximation in the modeling calculations, all  $HF(v)$  levels were assigned the  $T$ -dependence found for  $HF(1)$  and all  $DF(v)$  levels that found for  $DF(1)$ .

Table I demonstrates that the inverse rise times of the  $HF^\dagger$  and  $DF^\dagger$  fluorescence  $\tau_r^{-1}$  are given to an excellent approximation by  $k_1[H_2]$  and  $k_2[D_2]$ , respectively, at all temperatures studied. Plots of  $\tau_r^{-1}$  vs  $[H_2]$  and  $[D_2]$  are presented in Fig. 4. The resultant values of  $k_1$  and  $k_2$  obtained from a linear least squares fit to these data are presented in Table II as a function of temperature. The quoted errors in the individual  $k_1$  and  $k_2$  measurements represent the sum of the statistical error (1 $\sigma$ ) of the least squares fits in Fig. 4 and a systematic error of  $\pm 15\%$ , which primarily reflects measurement

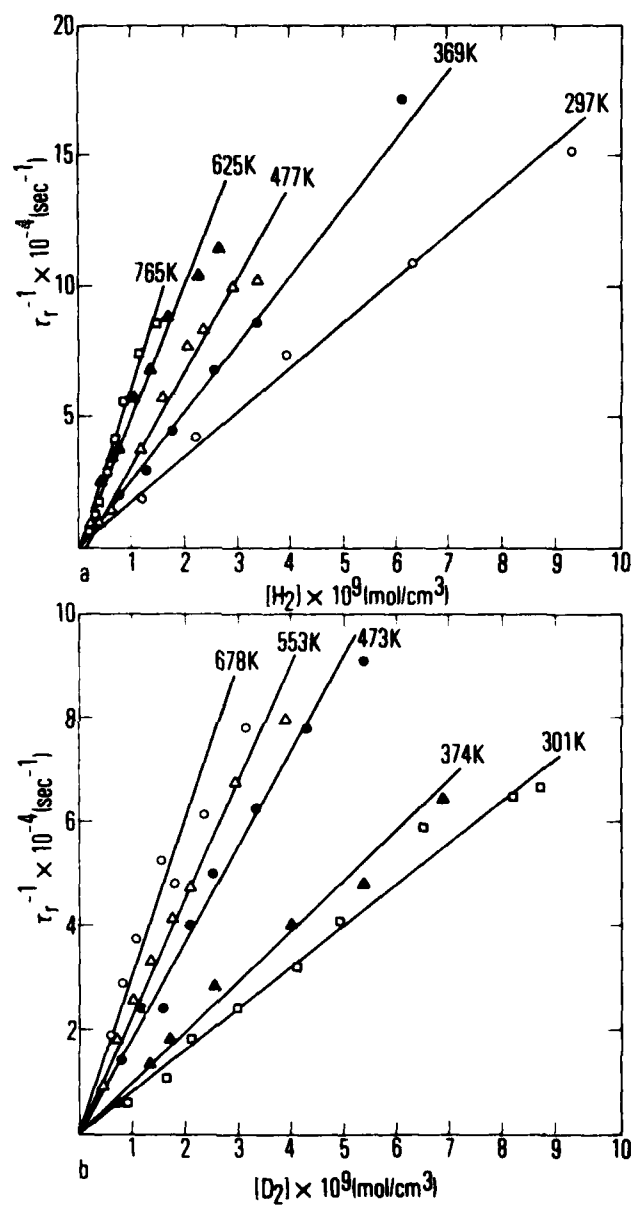


Fig. 4. Inverse rise times  $\tau_r^{-1}$  as a function of temperature for (a)  $\text{HF}^\dagger$  as a function of  $[\text{H}_2]$  and (b)  $\text{DF}^\dagger$  as a function of  $[\text{D}_2]$ .

TABLE II. Absolute rate coefficients as a function of temperature

$F + H_2 \xrightarrow{k_1} HF^\dagger + H$	
T(K)	$k_1(T)$ , $\text{cm}^3/\text{mol-sec}$
295	$(1.8 \pm 0.3) \times 10^{13}$
297	$(1.8 \pm 0.4) \times 10^{13}$
333	$(2.3 \pm 0.6) \times 10^{13}$
369	$(2.8 \pm 0.5) \times 10^{13}$
477	$(4.0 \pm 1.0) \times 10^{13}$
557	$(4.5 \pm 1.0) \times 10^{13}$
625	$(5.6 \pm 1.6) \times 10^{13}$
765	$(6.6 \pm 1.3) \times 10^{13}$
$F + D_2 \xrightarrow{k_2} DF^\dagger + D$	
T(K)	$k_2(T)$ , $\text{cm}^3/\text{mol-sec}$
295	$(9.5 \pm 1.7) \times 10^{12}$
301	$(8.6 \pm 1.7) \times 10^{12}$
332	$(1.2_5 \pm 0.3) \times 10^{13}$
374	$(1.0 \pm 0.2) \times 10^{13}$
401	$(1.3 \pm 0.6) \times 10^{13}$
473	$(1.8_5 \pm 0.4) \times 10^{13}$
553	$(2.2 \pm 0.5) \times 10^{13}$
678	$(2.9 \pm 0.7) \times 10^{13}$

errors in pressure, flow rates, and temperature. These data for  $k_1$  and  $k_2$  are plotted vs  $1/T$  in Fig. 5.

Over the temperature range studied ( $T = 295-795$  K), no non-Arrhenius behavior could be detected within the experimental uncertainty (see Sec. V). Thus, a least squares fit to the equation

$$\ln k = A - E_a/RT \quad (8)$$

was made using the transformation of statistical weights described by Cvetanovic et al.<sup>26,27</sup> Since all experimental values of  $k_1$  and  $k_2$  have a nearly constant fractional error, this is equivalent to performing an unweighted linear least squares of  $\ln k$  versus  $1/T$ . These Arrhenius plots yield the following values for  $k_1$  and  $k_2$ :  $k_1 = (1.3 \pm 0.25) \times 10^{14} \exp[-(1182 \pm 100)/RT]$ ;  $k_2 = (6.4 \pm 2.2) \times 10^{13} \exp[-(1200 \pm 142)/RT]$ ;  $k_{F+H_2}/k_{F+D_2} = (2.1 \pm 0.8) \exp[(18 \pm 250)/RT]$ .

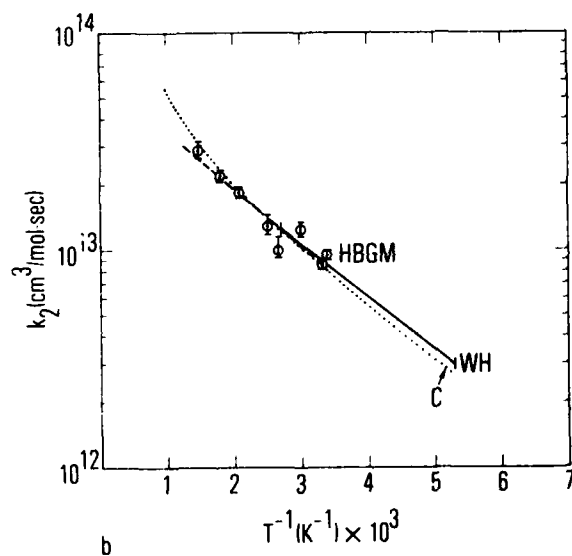
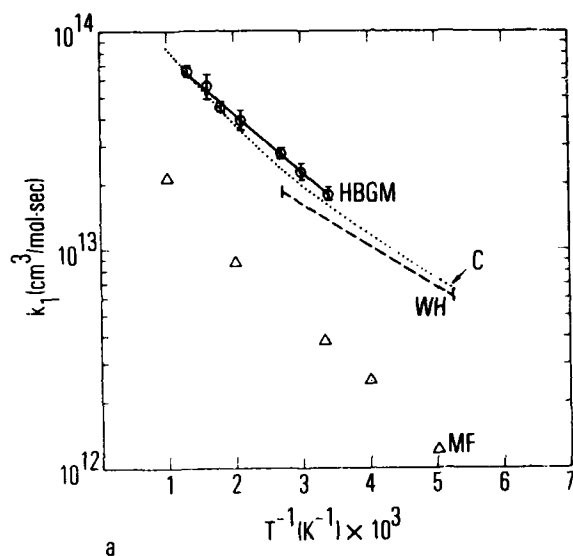


Fig. 5. Temperature dependence of the absolute reaction rates (a)  $k_1$ : HBGM (this work); WH (Ref. 6); C (Ref. 10); MF (Ref. 40); (b) HBGM (this work); WH (Ref. 6); C (Ref. 10).

## V. DISCUSSION

Room temperature data for  $F + H_2$  and  $F + D_2$  are reviewed in Ref. 1. Additional detail is given in the more comprehensive reviews of Refs. 2 through 5. Tables III and IV contain the Arrhenius parameters obtained for the  $F + H_2$  and  $F + D_2$  reactions, respectively. A variety of experimental methods has been employed; Wurzburg and Houston<sup>6</sup> also used the infrared multiphoton dissociation-infrared fluorescence technique in the complementary temperature regime of  $T = 190-373$  K. In this section, these two studies are compared, and the predicted ratio  $k_1/k_2$  is compared to very precise measurements made by Persky<sup>34</sup> and by Grant and Root.<sup>35</sup>

Table III and Fig. 5(a) clearly indicate a systematic error ( $\sim 30\%$ ) between the present data and the Wurzburg-Houston studies in the overlapping temperature range. Neither study has revealed the cause of this discrepancy. The agreement is much better for  $F + D_2$ , as indicated in Table IV and Fig. 5(b). Both studies deviate from the relative rate measurements  $k_1/k_2$  given by Persky<sup>34</sup> and by Grant and Root;<sup>35</sup> however, the deviations are rather slight. The recent low-temperature study by Bulatov<sup>31</sup> gives a  $k_1/k_2$  value in excellent agreement with Wurzburg and Houston.<sup>6</sup>

Figures 5(a) and 5(b) indicate the possibility of concave curvature to the Arrhenius plots for these two reactions. The exact one-dimensional quantum mechanical calculations by Schatz, Bowman, and Kuppermann for  $F + H_2$ <sup>35</sup> and  $F + D_2$ <sup>36</sup> predict concave non-Arrhenius behavior over the temperature range 200 to 1000 K on the basis of substantially different temperature dependencies for reaction into the various product vibrational channels. The experimental data of Perry and Polanyi<sup>15</sup> over the same temperature range do not agree with

TABLE III. Absolute temperature-dependent rate coefficients  
for  $F + H_2 \rightarrow HF + H$

$k_1$ , $\text{cm}^3/\text{mol-sec}$	Temperature range (K)	$k_1(295\text{K})$ , $\text{cm}^3/\text{mol-sec}$	Ref.
$1.6 \times 10^{14} \exp(-1600/RT)$	298-397	$1.05 \times 10^{13}$	28
$2.3 \times 10^{14} \exp(-1545/RT)^a$	298-397	$1.6_5 \times 10^{13}$	29
$1.6 \times 10^{14} \exp(-1190/RT)$	250-375	$2.1 \times 10^{13}$	29
$1.1 \times 10^{14} \exp(-1050/RT)$	260-370	$1.8_3 \times 10^{13}$	29
$9.3 \times 10^{13} \exp[-(1075 \pm 180)/RT]$	195-295	$1.5 \times 10^{13}$	30
$5.5 \times 10^{13} \exp[-(512 \pm 199)/RT]$	150-300	$2.3 \times 10^{13}$	31
$6.0 \times 10^{13} \exp[-(860 \pm 100)/RT]$	190-375	$1.4 \times 10^{13}$	6
$(1.3_6 \pm 0.25) \times 10^{14} \exp[-(1182 \pm 100)/RT]$	295-765	$1.8 \times 10^{13}$	this work

<sup>a</sup>Recalculation of Ref. 28 data.

TABLE IV. Absolute and relative temperature-dependent rate coefficients for  $F + D_2 \rightarrow DF + D$

$k_2$ , $\text{cm}^3/\text{mol-sec}$	$k_1/k_2$	Temperature Range (K)	$k_2(295\text{K})$ , $\text{cm}^3/\text{mol-sec}$	$k_1/k_2(295^\circ\text{K})$	Ref.
$4.9 \times 10^{13} \exp[-(795 \pm 179)/RT]$	$(1.48 \pm 0.22) \exp[(46 \pm 30)/RT]$	77-353		1.73	32
	$1.9 \exp(-280/RT)$	195-295	$1.2_6 \times 10^{13}$	0.73	30
	$(1.04 \pm 0.02) \exp[(378 \pm 10)/RT]$	163-417		$1.91 \pm 0.08$	33
	$(1.11 \pm 0.05) \exp[(358 \pm 26)/RT]$	303-475		$1.94 \pm 0.04$	34
	$(1.04 \pm 0.06) \exp[(377 \pm 12)/RT]$	273-457		$1.94 \pm 0.04$	35
$5.66 \times 10^{13} \exp[-(830 \pm 109)/RT]$	$0.98 \exp[(319 \pm 228)/RT]$	150-300	$1.3_7 \times 10^{13}$	1.68	31
$5.48 \times 10^{13} \exp[-(1100 \pm 100)/RT]$	$1.10 \exp[(240 \pm 200)/RT]$	190-373		1.66	6
$6.4 \times 10^{13} \exp[-(1200 \pm 142)/RT]$	$(2.1 \pm 0.8) \exp[(18 \pm 250)/RT]$	295-678	$(9.5 \pm 1.7) \times 10^{12}$	$2.17$ $1.92 \pm 0.23$	this work 1



this prediction. These data indicate extremely minor temperature variation of the important vibrationally-specific rate ratios  $k_1(3)/k_1(2)$  for  $F + H_2$ , and  $k_2(4)/k_2(3)$  or  $k_2(2)/k_2(3)$  for  $F + D_2$ . These one-dimensional calculations appear to be inadequate to describe the details of the temperature-dependent experimental reaction rates.

Transition state theory (TST) calculations performed by Cohen<sup>10</sup> indicate that curvature of this magnitude would be expected for either bent or linear intermediate F-H-H and F-D-D complexes, and sample curves have been superimposed in Figs. 5(a) and 5(b).

These TST calculations generally do not deal with a problem that has plagued classical trajectory studies of this system. Truhlar<sup>37</sup> and Muckerman and Newton<sup>38</sup> noted that  $F(^2P_{3/2})$  reacts with  $H_2$  on two doubly-degenerate potential surfaces in  $C_s$  symmetry. The lower ( $1\ ^2A'$ ) correlates with ground state products [ $HF(^1\Sigma) + H(^2S)$ ] while the upper ( $2A''$ ) correlates with excited-state  $HF[HF(^3\Pi) + H(^2S)]$  and will be nonreactive.

Similarly  $F(^2P_{1/2})$  interacts with  $H_2$  only on the  $2\ ^2A'$  surface that also correlates with electronically-excited products. In the absence of non-adiabatic transitions, one-half the collisions are potentially reactive if all the F atoms are in the  $^2P_{3/2}$  state. This value decreases to a limiting value of 1/3 as T is increased, thus populating the nonreactive  $^2P_{1/2}$  level. At intermediate temperatures, this multiple surface coefficient is described by

$$[\exp(-\Delta/kT) + 2]^{-1} \quad (9)$$

where  $\Delta$  is the spin orbit splitting in the F atom ( $404\text{ cm}^{-1}$ ). If  $F + H_2$  and  $F + D_2$  collisions are highly adiabatic, the above discussion indicates a

contribution to a convex Arrhenius plot. Tully<sup>39</sup> calculated contributions to nonadiabatic behavior arising both from a breakdown in the Born-Oppenheimer approximation and from spin-orbit coupling. The final result indicated that  $F(^2P_{1/2})$  was roughly 10% as reactive with  $H_2$  as was  $F(^2P_{3/2})$ . Thus, concern about the presence of the multiple potential surfaces seems warranted, and, based on Eq. (9), a pre-exponential factor less than or equal to one-third to one-half gas kinetic should not be surprising. In general, the Wurzburg-Houston study<sup>6</sup> and the present study are consistent with that interpretation. Muckerman and Faist<sup>40</sup> recently published a quasi-classical trajectory study for  $F + H_2$  that explicitly accounts for the multiple surface coefficient. The predicted pre-exponential is quite close to that found by Wurzburg and Houston.<sup>6</sup> The potential surface employed was the widely accepted "Muckerman 5," which has a barrier height of  $\sim 1.1$  kcal/mol; the resulting T-dependence of  $k_1$  indicates an activation energy substantially larger than that found by Wurzburg and Houston or the present study. Calculations on a surface with a slightly smaller barrier would provide an interesting comparison between theory and experiment.

Over the temperature range studied by Wurzburg and Houston and ourselves, arguments for non-Arrhenius behavior are ambiguous. The transition state theory calculations by Cohen<sup>10</sup> offer a plausible fit to the data; however, the transition state theory methodology is sufficiently flexible to allow a good fit by a number of different initial assumptions. Certain of these points have been recently reviewed.<sup>41</sup> The importance-sampling method used by Muckerman and Faist<sup>40</sup> should allow trajectory calculations of sufficient precision to test for non-Arrhenius behavior in the 200 to 1000 K range. We do

not believe that differences in the apparent  $E_a$  of  $\sim 250$  cal/mol should be dismissed as experimental artifacts given the wide temperature range studied.

In the temperature range 200 to 1000 K, between 65 and 55% of the energy of the  $F + H_2$  and  $F + D_2$  reactions ( $\sim 32$  kcal/mol) appears as product vibration.<sup>15</sup> Therefore, 35 to 45% of this energy ( $\sim 13$  kcal/mol) is available to heat the remaining reactants in an unbuffered laser mixture where the heat capacity  $C_v(T) = 6-7$  cal/mol K. Adiabatic temperature rises of 1000 to 2000 K are thus possible, even in the absence of vibrational relaxation. This problem is magnified in the  $H_2-F_2-O_2$  chain laser where the reaction  $H + F_2 \rightarrow HF(v) + F$  releases a substantial fraction of its exothermicity into translational and rotational degrees of freedom.

## VI. CONCLUSIONS

The infrared multiphoton dissociation-infrared chemiluminescence method has been applied to the measurement of absolute rates of  $F + H_2$  and  $F + D_2$  at elevated temperatures. The validity of using infrared chemiluminescence from  $HF^\dagger$  and  $DF^\dagger$  to monitor F-atom disappearance has been numerically modeled and verified. The results are in substantial agreement (although not completely for  $F + H_2$ ) with those of Wurzberg and Houston.<sup>6</sup> Rather than force a single Arrhenius equation to fit both the Wurzberg-Houston data and the present data, we have indicated that small differences in the reported activation energies in the 190 to 373 and 295 to 765 K temperature ranges are entirely plausible.

## REFERENCES

1. R. F. Heidner III, J. F. Bott, C. E. Gardner, and J. E. Melzer, *J. Chem. Phys.* 70, 4509 (1979).
2. W. E. Jones and E. G. Skolnik, *Chem. Rev.* 76, 563 (1976).
3. S. H. Mo, E. R. Grant, F. E. Little, R. G. Manning, C. A. Mathis, G. S. Werre, and J. W. Root, *Am. Chem. Soc. Symp. Ser.* 66, 59 (1978).
4. R. Foon and M. Kaufman, *Prog. React. Kinet.* 8, 81 (1975).
5. N. Cohen and J. F. Bott in Handbook of Chemical Lasers, ed. R.W.F. Gross and J. F. Bott (Wiley-Interscience, New York, 1976).
6. E. Wurzburg and P. L. Houston, "The Temperature Dependence of Absolute Rate Constants for the  $F + H_2$  and  $F + D_2$  Reactions" (submitted for publication).
7. J. T. Muckerman, *J. Chem. Phys.* 54, 1155 (1971); *J. Chem. Phys.* 56, 2997 (1972).
8. R. L. Jaffe and J. B. Anderson, *J. Chem. Phys.* 54, 2224 (1971).
9. R. L. Wilkins, *J. Chem. Phys.* 57, 912 (1972); *Mol. Phys.* 29, 555 (1975).
10. N. Cohen, private communication.
11. J. Whittier and J. J. T. Hough, private communication.
12. M. E. Riley and M. K. Matzen, *J. Chem. Phys.* 63, 4787 (1975).
13. A. Fontijn and W. Felder, *J. Phys. Chem.* 83, 24 (1979).
14. J. F. Bott and N. Cohen, *J. Chem. Phys.* 58, 4539 (1973).
15. E. B. Turner, G. Emanuel, and R. L. Wilkins, The NEST Chemistry Computer Program, TR-0059(6240-20)-1, The Aerospace Corporation, El Segundo, California (1970).
16. J. M. Herbelin and G. Emanuel, *J. Chem. Phys.* 60, 689 (1974).
17. D. S. Perry and J. C. Polanyi, *Chem. Phys.* 12, 419 (1976).

18. O. D. Krogh, D. K. Stone, and G. C. Pimentel, J. Chem. Phys. 66, 368 (1977).
19. J. F. Bott and R. F. Heidner, J. Chem. Phys. 66, 2878 (1977).
20. J. F. Bott, J. Chem. Phys. 65, 4239 (1976).
21. J. F. Bott and R. F. Heidner III, "Vibrational Relaxation of HF ( $v = 1$  and 3) in  $H_2$ ,  $N_2$ , and  $D_2$  at 200 and 295 K," submitted for publication.
22. D. J. Douglas and C. B. Moore, Chem. Phys. Lett. 57, 485 (1978).
23. P. Bado and H. van den Bergh, J. Chem. Phys. 68, 4188 (1978).
24. A. V. Nowack and J. L. Lyman, J. Quant Spectrosc. Radiat. Transfer 15, 945 (1975).
25. I. S. Fletcher and D. Husain, J. Chem. Soc. Faraday Trans. 2 74, 203 (1978).
26. R. J. Cvetanovic, D. L. Singleton, and G. Paraskevopoulos, J. Phys. Chem. 83, 50 (1979).
27. R. J. Cvetanovic and D. L. Singleton, Int. J. Chem. Kinet. IX, 481 (1977); IX, 1007 (1977).
28. K. H. Homann, W. C. Solomon, J. Warnatz, H. Gg. Wagner, and C. Zetzsch, Ber. Bunsenges. Phys. Chem. 74, 858 (1970).
29. J. Warnatz, H. Gg. Wagner, and C. Zetzsch, Report T-0240/92410/01017, Fraunhofer Gesellschaft (1972).
30. V. I. Igoshin, L. V. Kulahov, and A. I. Nikitin, Sov. J. Quantum Electron. 3, 306 (1974) (English edition); also in Kratk. Soobshch. Fiz. 1, 3 (1973) as reported in Chem. Abst. 79, 227 (1973).

31. V. P. Bulatov, V. P. Balakhnin, and O. M. Sarkisov, *Izv. Akad. Nauk. SSSR, Ser. Khim.* 8, 1734 (1977). English edition, *Bull. of the Acad. Sci. USSR* 26, 1600 (1977).
32. G. A. Kapralova, A. L. Margolin, and A. M. Chaikin, *Kinet. Katal.* 11, 810 (1970) (p. 669 in English edition).
33. A. Persky, *J. Chem. Phys.* 59, 3612 (1973)
34. E. R. Grant and J. W. Root, *Chem. Phys. Lett.* 27, 484 (1974); *J. Chem. Phys.* 63, 2970 (1975).
35. G. C. Schatz, J. M. Bowman, and A. Kuppermann, *J. Chem. Phys.* 63, 674 (1975).
36. G. C. Schatz, J. M. Bowman, and A. Kuppermann, *J. Chem. Phys.* 63, 685 (1975).
37. D. G. Truhlar, *J. Chem. Phys.* 56, 3189 (1972).
38. J. T. Muckerman and M. D. Newton, *J. Chem. Phys.* 56, 3191 (1972).
39. J. C. Tully, *J. Chem. Phys.* 60, 3042 (1974).
40. J. T. Muckerman and M. B. Faist, *J. Phys. Chem.* 83, 79 (1979).
41. D. G. Truhlar, *J. Phys. Chem.* 83, 188 (1979).

## LABORATORY OPERATIONS

The Laboratory Operations of The Aerospace Corporation is conducting experimental and theoretical investigations necessary for the evaluation and application of scientific advances to new military space systems. Versatility and flexibility have been developed to a high degree by the laboratory personnel in dealing with the many problems encountered in the nation's rapidly developing space systems. Expertise in the latest scientific developments is vital to the accomplishment of tasks related to these problems. The laboratories that contribute to this research are:

Aerophysics Laboratory: Launch vehicle and reentry aerodynamics and heat transfer, propulsion chemistry and fluid mechanics, structural mechanics, flight dynamics; high-temperature thermomechanics, gas kinetics and radiation; research in environmental chemistry and contamination; cw and pulsed chemical laser development including chemical kinetics, spectroscopy, optical resonators and beam pointing, atmospheric propagation, laser effects and countermeasures.

Chemistry and Physics Laboratory: Atmospheric chemical reactions, atmospheric optics, light scattering, state-specific chemical reactions and radiation transport in rocket plumes, applied laser spectroscopy, laser chemistry, battery electrochemistry, space vacuum and radiation effects on materials, lubrication and surface phenomena, thermionic emission, photosensitive materials and detectors, atomic frequency standards, and bioenvironmental research and monitoring.

Electronics Research Laboratory: Microelectronics, GaAs low-noise and power devices, semiconductor lasers, electromagnetic and optical propagation phenomena, quantum electronics, laser communications, lidar, and electro-optics; communication sciences, applied electronics, semiconductor crystal and device physics, radiometric imaging; millimeter-wave and microwave technology.

Information Sciences Research Office: Program verification, program translation, performance-sensitive system design, distributed architectures for spaceborne computers, fault-tolerant computer systems, artificial intelligence, and microelectronics applications.

Materials Sciences Laboratory: Development of new materials: metal matrix composites, polymers, and new forms of carbon; component failure analysis and reliability; fracture mechanics and stress corrosion; evaluation of materials in space environment; materials performance in space transportation systems; analysis of systems vulnerability and survivability in enemy-induced environments.

Space Sciences Laboratory: Atmospheric and ionospheric physics, radiation from the atmosphere, density and composition of the upper atmosphere, aurorae and airglow; magnetospheric physics, cosmic rays, generation and propagation of plasma waves in the magnetosphere; solar physics, infrared astronomy; the effects of nuclear explosions, magnetic storms, and solar activity on the earth's atmosphere, ionosphere, and magnetosphere; the effects of optical, electromagnetic, and particulate radiations in space on space systems.



DATE  
ILME  
—8